

Proposed flat-topped pulses bursts generation using all-pass multi-cavity structures

Miguel A. Preciado* and Miguel A. Muriel

ETSI Telecomunicacion, Universidad Politecnica de Madrid (UPM), 28040 Madrid, Spain.

*Corresponding author: ma.preciado@upm.es

Abstract: We propose a simple lossless method for the generation of flat-topped intensity pulses bursts from a single ultrashort pulse. We have found optimum solutions corresponding to different numbers of cavities and burst pulses, showing that the proposed all-pass structures of optical cavities, properly designed, can generate close to flat-topped pulse busts.

©2009 Optical Society of America

OCIS codes: (140.4780) Optical resonators; (140.3538) Lasers, pulsed; (230.1150) All-optical devices; (320.0320) Ultrafast optics; (350.4600) Optical engineering;

References and links

1. J. Caraquitená, Z. Jiang, D. E. Leaird, and A. M. Weiner, "Tunable pulse repetition-rate multiplication using phase-only line-by-line pulse shaping," *Opt. Lett.* **32**, 716-718 (2007).
2. C. -B. Huang and Y. Lai, "Loss-less pulse intensity repetition-rate multiplication using optical all-pass filtering," *IEEE Photon. Technol. Lett.* **12**, 167-169 (2000).
3. J. Azaña, "Pulse repetition rate multiplication using phase-only filtering," *Electron. Lett.* **40**, 449-451 (2004).
4. M. A. Preciado and M. A. Muriel, "Repetition-rate multiplication using a single all-pass optical cavity," *Opt. Lett.* **33**, 962-964 (2008).
5. M. A. Preciado and M. A. Muriel, "All-pass optical structures for repetition rate multiplication," *Opt. Express* **16**, 11162-11168 (2008).
6. M. A. Preciado and M. A. Muriel, "Repetition Rate Multiplication Using All-Pass Optical Structures," *Optics & Photonics News* **19**, 37-37 (2008).
7. J. Azaña and M. A. Muriel, "Temporal Talbot effect in fiber gratings and its applications," *Appl. Opt.* **38**, 6700-6704 (1999).
8. A. M. Weiner and D. E. Leaird, "Generation of terahertz-rate trains of femtosecond pulses by phase-only filtering," *Opt. Lett.* **15**, 51-53 (1990).
9. J. Azaña, R. Slavík, P. Kockaert, L. R. Chen, and S. LaRochelle, "Generation of Customized Ultrahigh Repetition Rate Pulse Sequences Using Superimposed Fiber Bragg Gratings," *J. Lightwave Technol.* **21**, 1490- (2003)
10. B. Muralidharan, V. Balakrishnan, and A. M. Weiner, "Design of Double-Passed Arrayed-Waveguide Gratings for the Generation of Flat-Topped Femtosecond Pulse Trains," *J. Lightwave Technol.* **24**, 586- (2006)
11. V. García-Muñoz, M. A. Preciado, and M. A. Muriel, "Simultaneous ultrafast optical pulse train bursts generation and shaping based on Fourier series developments using superimposed fiber Bragg gratings," *Opt. Express* **15**, 10878-10889 (2007)
12. A. Yariv and P. Yeh, "Wave propagation in periodic media," in *Photonics: Optical electronics in modern communications* (Oxford University Press, 2007).
13. J. Capmany, P. Muñoz, J.D. Domenech, and M. A. Muriel, "Apodized coupled resonator waveguides," *Opt. Express* **15**, 10196-10206 (2007).
14. J. Capmany and M. A. Muriel, "A new transfer matrix formalism for the analysis of fiber ring resonators: Compound coupled structures for FDMA," *J. Lightwave Technol.* **8**, 1904-1919 (1990).
15. A. Papoulis, *The Fourier Integral and Its Applications* (McGraw-Hill, New York, 1962).

1. Introduction

Researchers have explored several strategies for generating periodic pulse trains at repetition rates beyond those achievable by mode locking or direct modulation, since techniques for creating high repetition rate optical clock sources are highly sought after for future ultrahigh-speed optical communication systems. One alternative is the pulse repetition rate multiplication (PRRM) of a lower rate source, by filtering a periodic pulse train. Particularly,

phase-only filtering methods [1-7], mainly based on temporal Talbot effect [7], are highly desirable because of its high energy efficiency. Another method consists in generating optical pulse bursts from a single ultrashort pulse [8-11], with special interest in flat-topped envelope, and phase-only filtering methods [8,9].

In this Letter, we propose a method for generating flat-topped envelope optical pulse bursts of from a single ultrashort pulse using all-pass structures of optical cavities, where energy efficiency is nearly unity because of applying phase-only filtering. Here we consider structures composed of coupled cavities with practically same free spectral range (FSR), where two types of structures are proposed: partially reflecting coupled mirrors and coupled ring resonators waveguides (CROWs).

In the reminder of this Letter we present a method to find the optimum cavities parameters that lead to flat-topped burst envelope, and show the results for several numbers of burst pulses and cavities. In the examples, we design an optical structure based on a concrete solution, and show the results obtained from numerical simulations for several cases. Finally, we summarize and conclude our work.

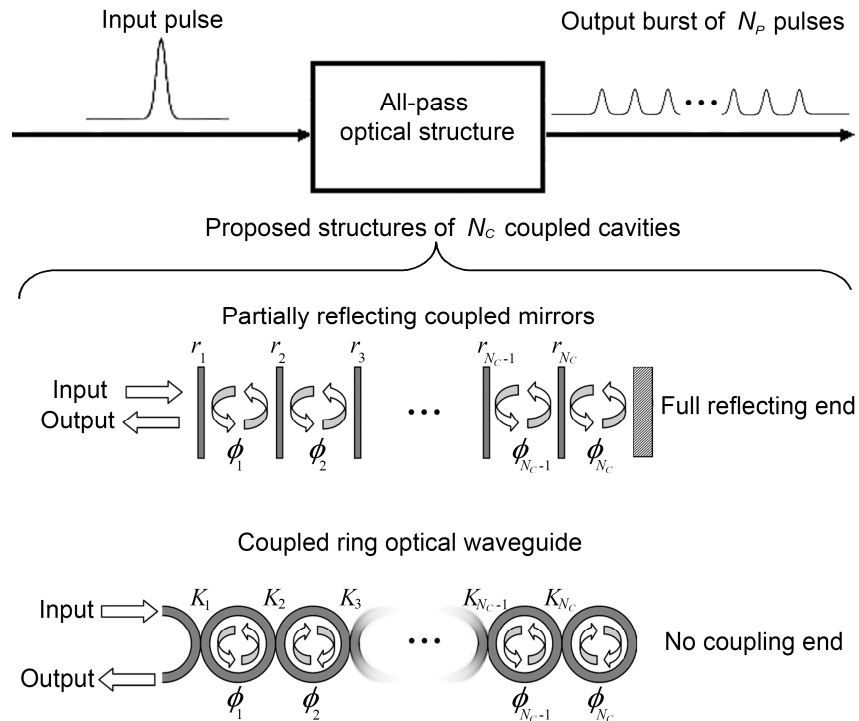


Fig. 1. Architecture of the system. A single short pulse is processed by the all-pass optical structure, generating an output burst of N_p pulses. Two kinds of coupled cavities structures are proposed, partially reflecting coupled mirrors and coupled ring optical waveguide.

2. Finding optimum solutions

An all-pass optical structure of lossless coupled cavities with similar free spectral ranges, as showed in Fig. 1, can be characterized by a set of $2 \times N_c$ parameters, where N_c is the number of cavities. In the case of mirrors based cavities, we can use the two sequences of N_c elements, $\{r_i\}$ and $\{\phi_i\}$, where r_i denotes the reflection coefficients corresponding to the i -th mirror, and ϕ_i denotes the round-trip phase corresponding to the i -th cavity. It is well known the equivalency of this structure with CROWs [12,13], using the relation:

$$K_i = 1 - r_i^2 \quad (1)$$

where K_i is the i -th coupling factor of the CROW. The impulse response of these optical structures, $h(t)$, can be obtained from inverse Fourier transform of the spectral response in reflection, $H(\omega)$, which can be calculated by applying the transfer matrix model method [12-14]. Since all the cavities have similar FSRs, we obtain a spectrally-periodic $H(\omega)$ with this same FSR too. Thus, we have a discrete-time function $h(t)$ that can be expressed as:

$$h(t) = \sum_{n=0}^{\infty} c_n \delta(t - nT) \quad (2)$$

where $T = \text{FSR}^{-1}$ is the period of the sequence, and c_n are complex coefficients which are function of the $2 \times N_C$ cavities parameters, i.e., $c_n = f(\{r_i\}, \{\phi_i\}, n)$. Moreover, we are interested in generating a sequence of N_p pulses of similar intensity from a single pulse. Let us define a causal discrete rectangular function of length N_p :

$$\text{rect}_{N_p}[n] = \begin{cases} 0, & n \leq 0 \\ 1, & 0 < n \leq N_p \\ 0, & n > N_p \end{cases} \quad (3)$$

Since $|c_n|^2$ define the envelope of the output burst intensity, we are interested in having a sequence $\{|c_n|^2\}$ similar to $\text{rect}_{N_p}[n]$ in order to have a flat-topped envelope. Let us define a figure of merit (FM) based on the normalized cross-correlation coefficient [15] to measure this similarity:

$$FM = \max \left[\frac{\sum_{n=1}^{\infty} |c_n|^2 \text{rect}_{N_p}(n+k)}{\sqrt{N_p \sum_{n=1}^{\infty} |c_n|^4}} \right], \quad k \in \mathbb{Z} \quad (4)$$

We are interested in the optimum set of $2 \times N_C$ parameters $\{r_i, \phi_i\}$ that maximize FM , for a certain number of desired burst pulses N_p , and a certain number of structure cavities N_C . Using a stochastic optimization algorithm, we have found optimum parameters for $N_C \in [2, 8]$ and $N_p \in [2, 20]$. Figure 2 shows a color map corresponding to the obtained optimum solutions where, in order to increase the contrast of the color map for of the best solutions, we do not represent FM directly, but a modified value obtained by $\log_{10}(1-FM)$. Accurate solutions correspond to low negative values, blue cells in the figure. If we compare the elements of a row in Fig. 2, corresponding to a concrete N_p value, we can see the monotonous behavior of the solutions. This means that adding a cavity can always improve the solution. However, if we compare the elements of a column corresponding to a concrete N_C value, no strictly monotonous or very regular behavior are necessarily observed, and the impossibility of obtaining a good solution for $N_p \gg N_C$ is the only evidence we can deduce. This shows that each N_p value defines an unrelated and independent optimization problem.

Table 1 shows two characteristic parameters of these solutions, the burst amplitude jitter (AJ), and extinction ratio (ER) of the burst, defined as:

$$\begin{aligned} AJ &= 20 \log_{10} \left(\frac{\max(|c_i|)}{\min(|c_j|)} \right) \\ ER &= 20 \log_{10} \left(\frac{\max(|c_i|)}{\max(|c_k|)} \right) \end{aligned} \quad (5)$$

where \log_{10} stands for the base 10 logarithm, $i \in [1, N_p]$, $j \in [1, N_p]$, and $k \in [N_p+1, \infty)$. Obviously, we are interested in solutions with low AJ and high ER values. It is worth noting that a different FM definition to Eq. (4) can be used, in other to get solutions with a different AJ and ER trade off. However, we have to take into account that the optimization algorithm convergence is also affected by the concrete FM definition.

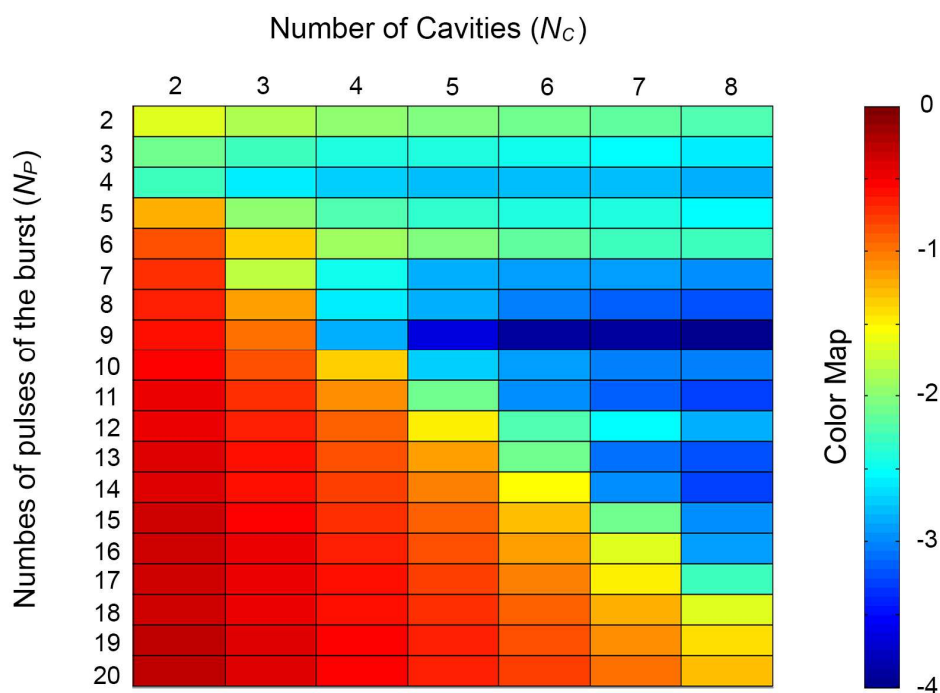


Fig. 2. False-color representation of $\log_{10}(1-FM)$, for a clear identification of accurate solutions, which correspond to the lowest negative values (blue cells).

Table 1. Pairs of $AJ \setminus ER$ values in decibels for optimum solutions with different N_C and N_P values.

| N_C | 2 | 3 | 4 | 5 | 6 | 7 | 8 |
|-------|---------|---------|---------|---------|---------|---------|---------|
| 2 | 0.08\7 | 0.04\8 | 0.04\9 | 0.04\10 | 0.02\10 | 0.03\10 | 0.01\11 |
| 3 | 0.25\8 | 0.14\10 | 0.11\10 | 0.08\11 | 0.08\12 | 0.07\11 | 0.03\11 |
| 4 | 0.09\9 | 0.07\12 | 0.08\12 | 0.09\12 | 0.10\12 | 0.04\14 | 0.05\13 |
| 5 | 4.42\13 | 0.62\9 | 0.19\8 | 0.18\10 | 0.08\11 | 0.18\11 | 0.5\12 |
| 6 | 13.1\14 | 2.81\4 | 0.25\7 | 0.19\8 | 0.14\9 | 0.12\10 | 0.09\10 |
| 7 | 11.9\14 | 2.18\8 | 0.52\9 | 0.14\12 | 0.12\13 | 0.11\12 | 0.11\12 |
| 8 | 15.5\18 | 11.2\8 | 0.31\8 | 0.12\11 | 0.09\12 | 0.08\12 | 0.08\13 |
| 9 | 18.4\17 | 10.9\15 | 0.71\15 | 0.08\15 | 0.03\16 | 0.02\16 | 0.02\17 |
| 10 | 17.3\18 | 11.7\17 | 8.70\16 | 0.19\10 | 0.19\11 | 0.13\11 | 0.11\12 |
| 11 | 18.2\22 | 15.0\19 | 7.43\13 | 1.54\12 | 0.08\10 | 0.11\13 | 0.08\14 |
| 12 | 21.3\22 | 16.5\24 | 10.6\12 | 5.29\12 | 1.06\8 | 0.11\12 | 0.08\12 |
| 13 | 21.7\23 | 20.3\20 | 12.7\13 | 6.54\13 | 1.74\12 | 0.20\12 | 0.15\13 |
| 14 | 23.3\26 | 20.4\21 | 17.9\12 | 8.23\14 | 4.80\10 | 0.26\11 | 0.20\12 |
| 15 | 25.5\27 | 20.7\24 | 17.6\20 | 10.6\16 | 7.00\15 | 1.74\12 | 0.22\12 |
| 16 | 26.6\28 | 25.5\24 | 20.9\20 | 13.3\17 | 8.21\15 | 4.14\9 | 0.21\10 |
| 17 | 28.2\30 | 25.6\29 | 22.3\19 | 15.2\15 | 8.19\14 | 3.85\16 | 1.25\9 |
| 18 | 30.0\32 | 28.5\29 | 23.6\19 | 14.8\18 | 11.8\13 | 6.80\18 | 2.83\10 |
| 19 | 31.5\33 | 28.6\31 | 24.0\26 | 16.9\19 | 11.4\22 | 9.15\18 | 4.78\9 |
| 20 | 33.0\35 | 30.9\32 | 27.5\26 | 18.5\21 | 23.5\22 | 14.1\20 | 6.24\12 |

3. Examples

We design a structure for an optimum solution corresponding to four cavities and nine pulses ($N_C=4$ and $N_P=9$). Since $AJ=0.71$ dB and $ER=15$ dB (see Table 1), a good trade-off between burst accuracy and structure complexity (only four cavities) is obtained. The structure

parameters of this solution are $\{r_i\}=\{0.339, 0.386, 0.483, 0.822\}$ and $\{\phi_i\}=\{0, 0.139, 0.023, -0.037\}$. For a CROW implementation, from Eq. (1) we can obtain $\{K_i\}=\{0.885, 0.851, 0.767, 0.325\}$. Let us assume an input Gaussian pulse with a full width at half maximum (FWHM) of 200 fs. In order to avoid pulses burst interference, we must impose $FSR_0^{-1}>200$ fs, where FSR_0 stands for the FSR of the structure. We choose $FSR_0^{-1}=1$ ps, i.e., $FSR_0=1$ THz (a length of cavity in the order of 100 μm), which, from Eq. (2), lead to an output pulse burst with a repetition rate of 1 THz. The different values of $\{\phi_i\}$ are obtained by very slight variations of the cavities FSR^{4,5}, i.e., $FSR_i=FSR_0\cdot(1+\varepsilon_i)$, where FSR_i is the exact value of the FSR of the i -th structure cavity, and ε_i is the relative variation of FSR_i regarding FSR_0 . Assuming a central frequency of $(\omega_0/2\pi)=193$ THz for the input signal, we can calculate^{4,5} $\{\varepsilon_i\}=10^{-3}\times\{0, -0.114, -0.019, 0.031\}$.

In order to illustrate the low dependence of this approach to variations on the central frequency of the input signal, we have also simulated the previous structure assuming an input pulse of same width at a different central frequency, $(\omega_0'/2\pi)=195$ THz. The output pulses burst obtained from a numerical simulation of the designed structure for both input signals are represented in Fig. 3, where practically identical outputs can be observed.

It is worth noting that, in these examples, we have supposed ideal lossless cavities. In case of CROW structures, the ring resonators losses due to scattering or bending may be significant. Table 2 show how the cavity losses affect to the structure performance in terms of FM , AJ , ER , and energy efficiency (EE), considering several values of round-trip power loss ($RTPL$) of each cavity, assuming same $RTPL$ for all the cavities of the structure. As expected, the energy efficiency and the pulse train uniformity decrease with the cavity losses. Moreover, the CROW dispersion may be significant for a 200 fs pulse, which affect as a increasing of the pulse width and a distortion of the pulse shape.

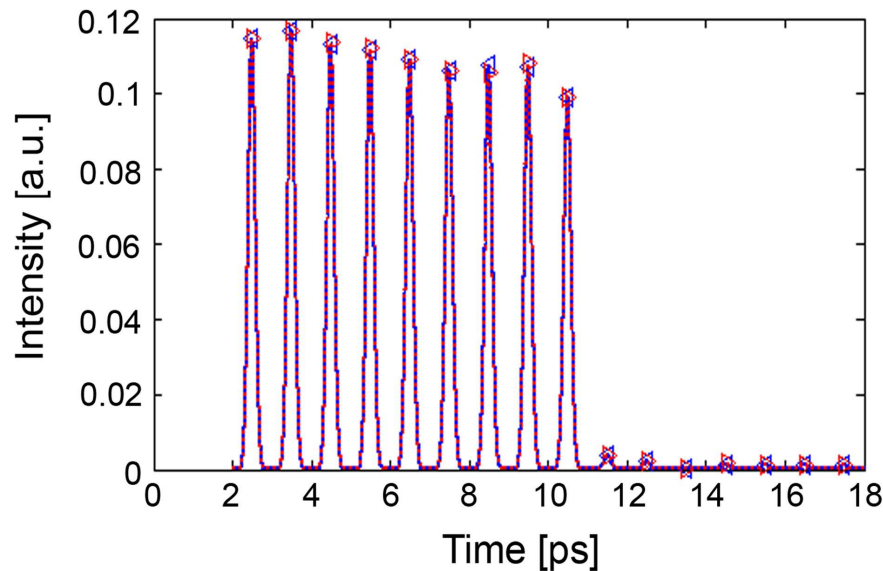


Fig. 3. Output burst of 9 pulses obtained from a numerical simulation of the designed optical structure with an input 200 fs FWHM gaussian pulse at 193 THz (blue-solid line), and at 195 THz (red-dotted line), hardly distinguishable. The maximums of each pulse are marked with a blue left-pointing triangle for the first input, and with a red right-pointing triangle for the second one, appearing a six-point star where both coincide.

Table 2. Performance of the designed structure in terms of figure of merit, amplitude jitter, extinction ratio, and energy efficiency, considering several values of round-trip power losses (*RTPL*).

| <i>RTPL</i> (%) | Figure of merit | Amplitude jitter (dB) | Extinction ratio (dB) | Energy efficiency (%) |
|-----------------|-----------------|-----------------------|-----------------------|-----------------------|
| 0 | 0.9988 | 0.71 | 14.7 | 100 |
| 0.5 | 0.9981 | 0.87 | 14.9 | 98.0 |
| 1 | 0.9975 | 1.02 | 15.1 | 96.1 |
| 2 | 0.9953 | 1.35 | 15.4 | 92.4 |
| 3 | 0.9926 | 1.71 | 15.8 | 88.8 |
| 4 | 0.9891 | 2.07 | 16.2 | 85.5 |
| 5 | 0.9850 | 2.43 | 16.6 | 82.2 |

4. Conclusion

We have proposed all-pass optical structures composed of coupled cavities for the generation of flat-topped intensity pulse bursts with high energetic efficiency (ideally 100% for lossless cavities). We have obtained the optimum parameters for 2-to-8 cavities and 2-to-20 pulses, where accurate solutions have been found. Two different implementations of coupled cavities are proposed, partially reflecting coupled mirrors and CROWs. The choice depends on the concrete application, taking into account that CROWs non-idealities, mainly cavities losses, may have a significant effect in the output. In the examples, we have obtained readily feasible cavities parameters, and we have simulated the optical structure for inputs of different central frequency. We have showed the low dependence of this approach to frequency variations of the input source. Thus, unlike most of cavities filtering PRM techniques, the system does not require the locking of the spectrum of the input signal to the spectral response of the optical structure.

Acknowledgements

This work was supported by the Ministerio de Ciencia e Innovacion of Spain under Project "Plan Nacional de I+D+I TEC2007-68065-C03-02".